Carcinogenesis, 2015, Vol. 36, No. 11, 1388–1396

doi:10.1093/carcin/bgv120
Advance Access publication August 29, 2015
Original Manuscript

ORIGINAL MANUSCRIPT

Akkermansia muciniphila and *Helicobacter typhlonius* modulate intestinal tumor development in mice

Celia Dingemanse, Clara Belzer[1], Sacha A.F.T.van Hijum[2,3], Marie Günthel, Daniela Salvatori[4,5], Johan T. den Dunnen, Ed J.Kuijper[6], Peter Devilee, Willem M.de Vos[1,7], GertJan B.van Ommen, and Els C.Robanus-Maandag*

Department of Human Genetics, Leiden University Medical Center 2333 ZC, Leiden, The Netherlands, [1]Laboratory of Microbiology, Wageningen University 6703 HB, Wageningen, The Netherlands, [2]Centre for Molecular and Biomolecular Informatics Bacterial Genomics, Radboud University Medical Centre 6525 GA, Nijmegen, The Netherlands, [3]NIZO Food Research BV 6718 ZB, Ede, The Netherlands, [4]Department of Anatomy and Embryology, [5]Central Animal Facility and [6]Department of Medical Microbiology, Leiden University Medical Center 2300 RC, Leiden, The Netherlands and [7]Department of Veterinary Biosciences, University of Helsinki 00014, Helsinki, Finland

*To whom correspondence should be addressed. Tel: +31 71 5269511; Fax: +31 71 5268285; Email: e.c.robanus@lumc.nl

Abstract

Gastrointestinal tumor growth is thought to be promoted by gastrointestinal bacteria and their inflammatory products. We observed that intestine-specific conditional *Apc* mutant mice (Fabpl*Cre*;*Apc*$^{15lox/+}$) developed many more colorectal tumors under conventional than under pathogen-low housing conditions. Shotgun metagenomic sequencing plus quantitative PCR analysis of feces DNA revealed the presence of two bacterial species in conventional mice, absent from pathogen-low mice. One, *Helicobacter typhlonius*, has not been associated with cancer in man, nor in immune-competent mice. The other species, mucin-degrading *Akkermansia muciniphila*, is abundantly present in healthy humans, but reduced in patients with inflammatory gastrointestinal diseases and in obese and type 2 diabetic mice. Eradication of *H.typhlonius* in young conventional mice by antibiotics decreased the number of intestinal tumors. Additional presence of *A.muciniphila* prior to the antibiotic treatment reduced the tumor number even further. Colonization of pathogen-low Fabpl*Cre*;*Apc*$^{15lox/+}$ mice with *H.typhlonius* or *A.muciniphila* increased the number of intestinal tumors, the thickness of the intestinal mucus layer and *A.muciniphila* colonization without *H.typhlonius* increased the density of mucin-producing goblet cells. However, dual colonization with *H.typhlonius* and *A.muciniphila* significantly reduced the number of intestinal tumors, the mucus layer thickness and goblet cell density to that of control mice. By global microbiota composition analysis, we found a positive association of *A.muciniphila*, and of *H.typhlonius*, and a negative association of *unclassified Clostridiales* with increased tumor burden. We conclude that *A.muciniphila* and *H.typhlonius* can modulate gut microbiota composition and intestinal tumor development in mice.

Introduction

In the human intestine, the 10^{14} microbial organisms (at least 160 species) normally participate in a symbiotic relationship with their host (1,2). Intestinal microbes protect against enteropathogens, extract nutrients and energy from diets and contribute to normal immune function (2). Disruptions to the normal balance between the intestinal microbiota and the host can have detrimental effects on host physiology contributing to susceptibility for diseases such as obesity, fatty liver disease, type 1 and 2 diabetes and kidney disease (3). Moreover, microbes in the gastrointestinal tract can promote tumor development. This is clearly illustrated by the fact that chronic gastritis due to *Helicobacter pylori* in the stomach increases the

Received: March 21, 2015; **Revised:** July 22, 2015; **Accepted:** August 13, 2015

Abbreviations

CRC	colorectal cancer
NF	normal food
PBS	phosphate-buffered saline
PCA	principal component analysis
qPCR	quantitative polymerase chain reaction

risk of sporadic gastric adenocarcinoma (4). Consequently, eradication of *H.pylori* by antibiotic treatment is regarded as a primary chemoprevention strategy to reduce gastric cancer incidence in man.

There is accumulating evidence that members of the gut microbiota are also involved in intestinal diseases such as inflammatory bowel disease, comprising both ulcerative colitis and Crohn's disease, and colorectal cancer (CRC) (5). Because chronic inflammation represents a significant CRC risk factor, most studies focused on the small subset of colitis-associated colorectal cancers, and are based on mouse models. Colitis-prone mice, when treated with antibiotics or derived into germ-free conditions, were devoid of intestinal inflammation and colorectal tumors (6,7). More specifically, two human pathogens have been implicated in colitis-associated colorectal tumors, enterotoxigenic *Bacteroides fragilis* and *Escherichia coli* (8,9). The non-human enteric pathogens *H.hepaticus* and *H.bilis* can also induce colitis-associated colonic tumors in immunocompromised mice via upregulation of proinflammatory mediators (10–14).

Intestinal microbiota may also influence the development of non-colitis-associated CRC. This was shown in $Apc^{Min/+}$ mice, developing significantly fewer intestinal tumors under germ-free as compared to specific pathogen-free conditions (15). This indicates that commensal bacteria are not required for, but can potentiate tumorigenesis independent of chronic inflammation. Recently, due to the development of unbiased high-throughput sequencing, details of the composition of the human CRC-associated microbiome are emerging (16). Based on metagenomic analyses of CRC and adjacent normal tissues, overrepresentation of the periodontal pathogen *Fusobacterium nucleatum* in CRC was reported (17–19). This species was recently shown to promote non-colitis-associated intestinal tumorigenesis in $Apc^{Min/+}$ mice (20).

$Apc^{Min/+}$ mice and other mouse models heterozygous for truncating mutant *Apc* alleles develop large numbers of intestinal tumors due to functional loss of the wild-type allele, thereby mimicking the hereditary colorectal tumor syndrome familial adenomatous polyposis. However, the murine tumors mainly occur in the small intestine. Our conditional *Apc* mutant Fabpl*Cre*;$Apc^{15lox/+}$ mice, which are functionally wild-type for *Apc* in all cells except Fabpl*Cre*-expressing epithelial cells of the distal small and large intestine develop tumors predominantly in the large intestine as in human familial adenomatous polyposis-related and sporadic colorectal cancer (21). Fabpl*Cre*;$Apc^{15lox/+}$ mice, like $Apc^{Min/+}$ mice, develop non-colitis-associated intestinal tumors (11,15,20,22).

In this study, we investigated whether a decreased frequency of colon tumors in Fabpl*Cre*;$Apc^{15lox/+}$ mice under pathogen-low housing conditions, as compared to conventional (i.e. pathogen higher) housing conditions, could be attributed to specific changes in intestinal microbial composition. We found two bacterial species, *H.typhlonius* and *Akkermansia muciniphila*, to be specifically associated with conventional housing. We tested their intestinal tumor-modulating role by eradicating them from conventional Fabpl*Cre*;$Apc^{15lox/+}$ mice and by introducing them in pathogen-low Fabpl*Cre*;$Apc^{15lox/+}$ mice.

Materials and methods

Bacterial strains and culturing

H.typhlonius (CCUG 48335T) was grown microaerobically (6% oxygen in a mixture of 10% carbon dioxide, 10% hydrogen and 80% nitrogen) on Biomerieux chocolate agar + PolyViteX (PVX) plates (Mediaproducts, Groningen, The Netherlands) for 2–3 days at 37°C (23,24). *A.muciniphila* MucT (ATTC BAA-835) was grown anaerobically in a basal mucin-based medium (25).

Mice, cohousing, antibiotic treatment and oral gavage

All experiments on Fabpl*Cre*;$Apc^{15lox/+}$ and $Apc^{15lox/+}$ mice in a C57BL/6 background were performed in accordance with institutional and national guidelines and regulations (21). Treatment groups included equal numbers of males and females. Mice were housed under conventional conditions in open cages, or, after initial rederivation of the Fabpl*Cre* and $Apc^{15lox/+}$ strains, under pathogen-low FELASA+ conditions in individually ventilated cages. Both conventional and pathogen-low mice received irradiated standard RM3 (P) food pellets (SDS, Essex, UK). Pathogen-low mice were provided with sterile water.

The conventional condition was maintained through cohousing of conventional mice with newly generated pathogen-low mice in individually ventilated cages, resulting in cross-contamination by coprophagy, followed by generation of conventional offspring in individually ventilated cages.

For ablation of *Helicobacter*, an antibiotic cocktail of amoxicillin (600 mg/kg), metronidazole (200 mg/kg), and clarithromycin (100 mg/kg), combined with omeprazole (4 mg/kg) in standard food pellets was used (26). In the colonization experiment, mice were pretreated with this antibiotic cocktail for 1 week at 3 weeks of age. Inoculations by oral gavages started 4 days later. Per gavage, 4×10^6 colony-forming units (cfus) *H.typhlonius* in 0.2 ml Brucella broth + 20% glycerol were administered, or 10^9 cfus *A.muciniphila* in 0.1 ml phosphate-buffered saline (PBS)-diluted anaerobic glycerol stock (27). Bacterial colonization was validated in the feces by quantitative PCR (see below). Weight was measured every 2 weeks and feces samples were aseptically collected in liquid nitrogen and stored at –80°C until further processing.

Histological analysis

Tissues were fixed in 4% neutral buffered formalin, embedded in paraffin, sectioned and stained with H&E. Tumor numbers were based on tumors ≥1 mm. Histopathological analysis of the tumors was performed as described previously (21). The degree of colitis was scored by one of the authors (D.S.), who was blinded to the genotype and experimental protocols used. Each of four histologic parameters were scored as absent (0), mild (1), moderate (2) or severe (3): mononuclear cell infiltraton, polymorphonuclear cell infiltration, epithelial hyperplasia and epithelial injury. A score ≥5 is indicative of colitis (6).

Mucus layer thickness analysis and goblet cell counting

Colonic tissues were submerged in methanol-Carnoy's fixative (60% methanol, 30% chloroform, 10% glacial acetic acid) for 1 week. After processing and embedding in paraffin, 5 µm transverse sections were stained with alcian blue at pH 2.5 and periodic acid-Schiff (AB/PAS). Stained sections were scanned using the Philips Digital Pathology Solution (Philips, Best, The Netherlands). Digital images were analyzed with Image J (http://imagej.nih.gov/ij/). The inner mucus layer thickness was measured perpendicular to this layer at 24 positions at equal distances starting from a randomly selected position per section per mouse without prior knowledge of the sample type.

Fecal DNA isolation, commercial screening

DNA was extracted from frozen fecal samples using the MOBIO Ultraclean Fecal kit (Sanbio, Uden, The Netherlands). Commercial screening for the detection of bacterial pathogens (*Citrobacter rodentium*, *Corynebacterium kutscheri*, *Pasteurellaceae*, *Salmonella* spp., *Streptococci* (β-hemolytic), *Streptococcus pneumoniae*, *Streptobacillus morilliformis*, *Helicobacter* spp.,

H.typhlonius, *H.hepaticus* and *H.bilis*) was performed by QM Diagnostics (Nijmegen, The Netherlands).

Metagenomic sequencing and phylogenetic profiling

Genomic DNA libraries were prepared from 1 to 2 µg fecal DNA according to the Illumina protocol. Single-end shotgun metagenomic sequencing was performed using the Illumina Genome Analyzer I (Illumina, San Diego, CA) as described previously (28).

The pathogen-low sample consisted of 7 200 416 50-nucleotide reads and the conventional sample of 8 142 725 reads. Reads with undefined nucleotides were removed, resulting in 7 185 910 reads for the pathogen-low sample and 8 046 334 reads for the conventional sample. Reads were aligned to the non-redundant database (downloaded from https://www.ncbi.nlm.nih.gov/Ftp/ at the 31st of March 2010) with BLAST using BLASTx with the following parameters: blastall -p blastx -Q11 –a1 –F 'm S' -d nr –I <input> -m7 -<output> (29). The BLASTx alignment results were loaded in MEGAN software (version 3.8) for taxonomy assignment, resulting in a file containing the taxonomy-assigned reads (30). A hit should have a minimum blast score of 25 and only the top 20% hits with this score threshold was taken into account. A minimum of three hits was required to support an assignment to a given taxonomy node. Almost 21% of the reads of the conventional sample and 33% of the reads of the pathogen-low sample received taxonomic assignment. Cytoscape software (http://www.cytoscape.org/) was used to visualize the differences between taxonomy-assigned reads of both fecal DNA samples.

Quantitative polymerase chain reaction

Each quantitative polymerase chain reaction (qPCR) was performed in 10 µl according to standard procedures using 0.5 µl EvaGreen (Biotium, Hayward, CA), 0.5 unit FastStart Taq DNA polymerase (Roche Applied Science, Mannheim, Germany) and primer sets for *H.typhlonius* (forward 5′-AGGGACTCTTAAATATGCTCCTAGAGT-3′; reverse 5′-ATTCATCGTGTTTGAATGCGTCAA-3′, yielding a 123 bp product) and for *A.muciniphila* (forward 5′-CAGCACGTGAAGGTGGGGAC-3′; reverse 5′-CCTTGCGGTTGGCTTCAGAT-3′, yielding a 329 bp product) (31,32). Triplicate qPCR reactions were analyzed on the LightCycler 480 (Roche). Standard curves were created using serial 10-fold dilutions of *H.typhlonius* or *A.muciniphila* pure culture DNA corresponding to 10 ng/µl. The bacterial concentration of each sample was calculated by comparing the crossing point (Cp) values obtained from the standard curve. Definition of the upper limit for absence of the bacteria was based on qPCR data of a large series of fecal samples of pathogen-low mice in the breeding facility.

MITChip microarray analyses

The phylogenetic Mouse Intestinal Tract Chip (MITChip) microarray consists of 3580 different oligonucleotide probes that target the V1 and V6 hypervariable regions of the microbial 16S rRNA gene. MITChip analysis was performed as previously described (27,33,34).

Statistical analyses

Generally, data were displayed in bar graph format, with the standard error of the mean (SEM) represented by the error bars. Data were significantly different according to *post hoc* ANOVA one-way statistical analysis, unless otherwise specified.

Results

Intestinal tumor number depends on housing conditions

We observed that Fabpl*Cre*;*Apc*$^{15lox/+}$ mice, raised under new pathogen-low conditions, displayed a strongly reduced mean frequency of colorectal tumors (17%) in comparison to mice raised under old conventional housing conditions (63%) (Figure 1A). Such a reduction is potentially clinically relevant. Therefore, we established new 'conventional mice' by cohousing pathogen-low mice in individually ventilated cages in the new pathogen-low facility with mice that had been conventionally housed previously. We housed these new conventional and pathogen-low mice for 22 weeks under pathogen-low conditions. The pathogen-low Fabpl*Cre*;*Apc*$^{15lox/+}$ mice displayed significantly fewer intestinal tumors (27%) as compared to the conventional mice (mean of 21.4 and 29.5, respectively, $P < 0.01$, Figure 1B).

Conventional and pathogen-low mice differ in gut microbiome composition

We hypothesized that a housing-related difference in gut microbiota led to the reduced intestinal tumors in pathogen-low Fabpl*Cre*;*Apc*$^{15lox/+}$ mice. To investigate this, feces of two conventional and two pathogen-low *Apc*$^{15lox/+}$ mice were commercially screened for the presence of bacterial pathogens. qPCR analysis indicated the presence in the conventional samples only of the species *H.typhlonius*, but not *H.hepaticus* or *H.bilis* (data not shown).

Since only pathogenic bacteria were included in the commercial screening, we performed shotgun metagenomic sequencing to compare the complete bacterial profiles of independent feces samples. Total DNA of a conventional and pathogen-low feces sample was used to generate, respectively, 5.0 and 9.4 Gb of sequence with the Genome Analyzer I (Illumina). Of the mapped reads, 392 548 (4.8% of total) and 391 717 (5.4% of total) could be assigned to bacterial sequences in the conventional and pathogen-low sample (Supplementary Table 1, available at *Carcinogenesis* Online). Taxa were selected that showed at least a 20-fold difference in assigned reads between both samples and at least 1000 reads in either.

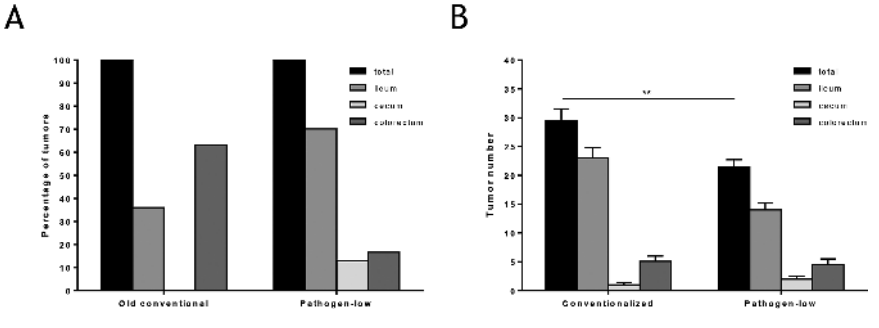

Figure 1. Intestinal tumor numbers depend on housing conditions. (**A**) Percentages of intestinal tumors in Fabpl*Cre*;*Apc*$^{15lox/+}$ mice of 5–7.5 months of age housed under old conventional and under pathogen-low conditions. (**B**) Intestinal tumor numbers of conventionalized and pathogen-low Fabpl*Cre*;*Apc*$^{15lox/+}$ mice of 22 weeks of age housed under pathogen-low conditions. Mean tumor numbers ± SEM are shown. Data are significantly different according to *post hoc* ANOVA one-way statistical analysis. $^{**}P < 0.01$.

Under these criteria, only taxa of the phyla *Proteobacteria* and *Verrucomicrobia* were overrepresented in the conventional sample (Figure 2A and Supplementary Table 1, available at *Carcinogenesis* Online). Within *Proteobacteria*, the genus *Helicobacter* was responsible for the overrepresentation, in line with the commercial screening (Figure 2A and Supplementary Table 1, available at *Carcinogenesis* Online). Commercial, species-specific *Helicobacter* qPCR on both sequenced samples confirmed the earlier findings.

Within the phylum *Verrucomicrobia*, the genus *Akkermansia* was responsible for the overrepresentation in the conventional sample. This genus is known to have a single representative, *A.muciniphila* (Figure 2A and Supplementary Table 1, available at *Carcinogenesis* Online) (35,36).

To independently compare the global microbiota composition of the conventional and pathogen-low feces samples, we performed phylogenetic microarray analysis using the MITChip on four samples of each category (34). Hierarchical cluster analysis demonstrated that the conventional and pathogen-low samples clustered separately (Figure 2B). Principal component analysis (PCA) revealed that members of *unclassified Clostridiales* correlated with pathogen-low housing. Among the taxa associated with conventional housing were *A.muciniphila* and *Helicobacter* (Figure 2C). qPCR of an extended series of conventional and pathogen-low samples revealed that, relative to pathogen-low mice, conventional mice showed on average a ~70 000-fold increase in *H.typhlonius* and a ~7000-fold increase in *A.muciniphila* (Figure 2D). Our data on the increased presence of *H.typhlonius* and *A.muciniphila* in conventional mice and the concomitant increase of intestinal tumors suggested that these two bacterial species were good candidates for microbiota-dependent intestinal tumor modulation.

Antibiotic treatment reduces intestinal tumor development

To investigate a potential relationship between the presence of *H.typhlonius* in the gut and intestinal tumor formation, the microbiota associated with the conventional condition was transferred to parental pathogen-low mice by 1 week of cohousing with conventional mice before breeding. Offspring mice were subdivided in three cohorts of both Fabpl*Cre*;*Apc*$^{15lox/+}$ test and *Apc*$^{15lox/+}$ control mice. One cohort remained untreated [defined as normal food (NF) cohort]. The other two cohorts were treated with antibiotics (Abx: amoxicillin, metronidazole and clarithromycin, combined with omeprazole) in their food pellets to eradicate *Helicobacter* (Figure 3A). One of these was treated from 4 to 13 weeks of age (Abx pup cohort). In the other, treatment started already at embryonic day 11.5 via the pregnant mother, and continued up to 4 weeks of age (Abx embryo cohort). Indeed, *H.typhlonius* was eradicated by the antibiotic treatment as shown for the Abx pup cohort (Supplementary Figure 1A, available at *Carcinogenesis* Online). At 22 weeks of age, all *Apc*$^{15lox/+}$ control mice developed on average 0.26 intestinal tumors per mouse, while Fabpl*Cre*;*Apc*$^{15lox/+}$ mice of the NF cohort developed on average 29.5 intestinal tumors (Figure 3B). After antibiotic treatment, the intestinal tumor count of both the Abx pup and Abx embryo cohort was significantly decreased to a mean of 18.4 ($P = 0.003$) and 20.1 ($P = 0.013$) tumors per mouse, whereas no difference was seen between the two regimens ($P = 0.63$)

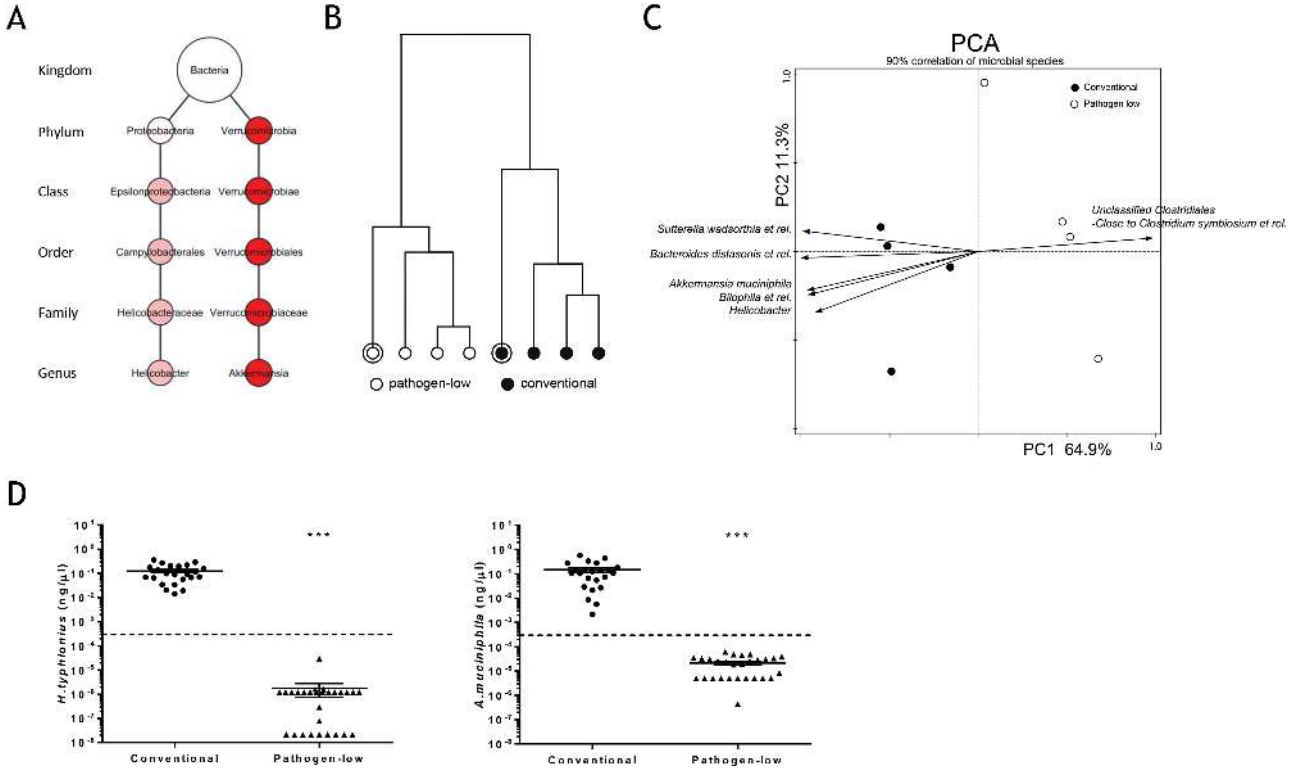

Figure 2. Overrepresentation of *Helicobacter* and *Akkermansia* in conventionally housed mice. (**A**) Comparison of taxonomy-assigned read numbers of metagenomically sequenced fecal DNA samples of a conventionally and pathogen-low housed *Apc*$^{15lox/+}$ mouse. Taxa are shown with ≥ 20-fold difference in read number between both samples and ≥1000 assigned reads in either. Light-red, ~40-fold, and dark red, ~140-fold difference. (**B**) Hierarchical clustering of MITChip data from pathogen-low and conventional mice (Pearson correlation). Circles indicate metagenomically sequenced samples. (**C**) PCA using the MITChip data of (B). (**D**) Fecal concentrations of *H.typhlonius* and *A.muciniphila* in conventionally and pathogen-low housed mice ($n = 23$ and 28, respectively) by qPCR analysis. Mean concentrations (center lines) ± SEM (error bars) are shown. ***$P < 0.001$. Dashed line indicates defined upper limit for absence of bacteria.

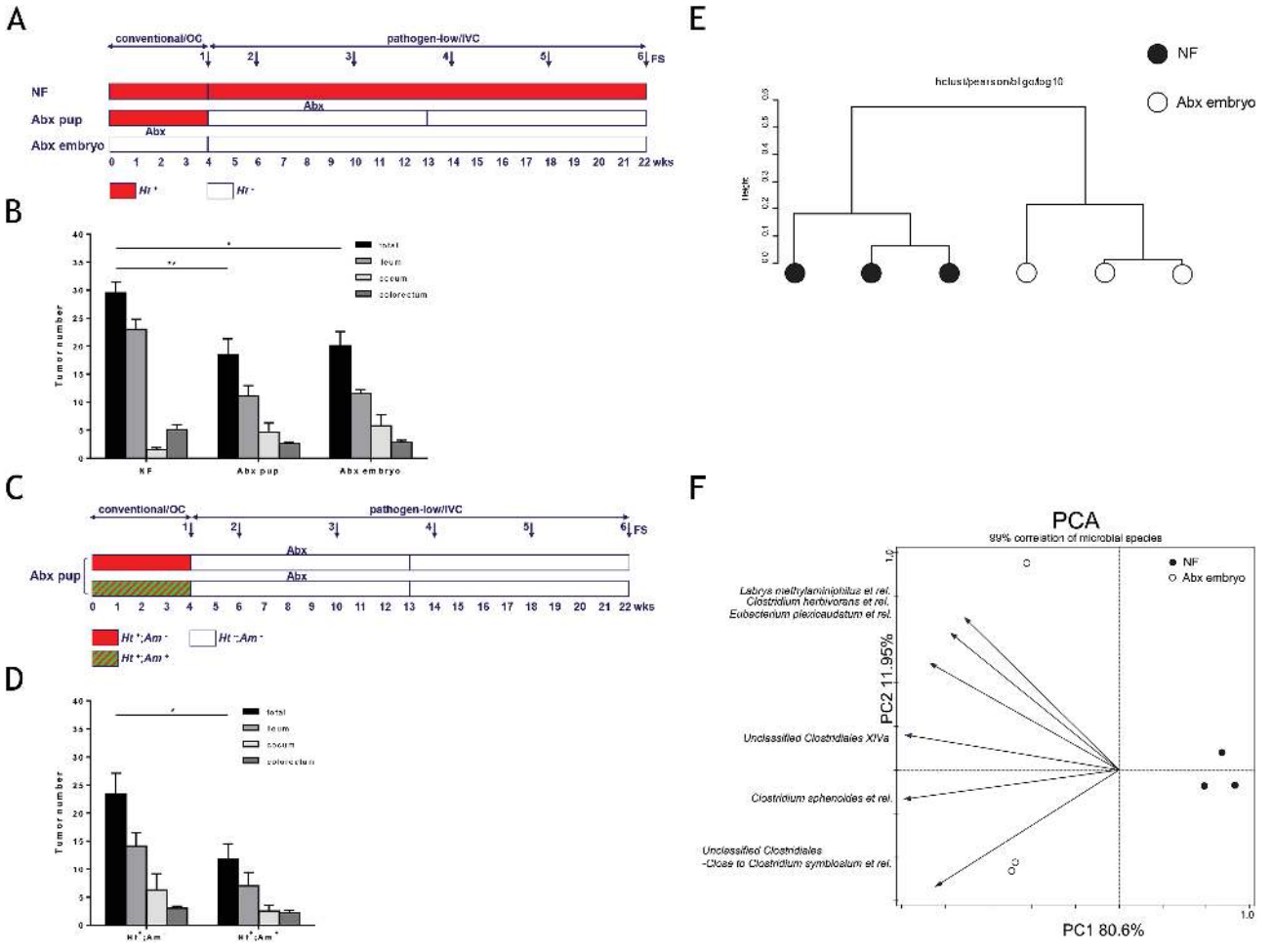

Figure 3. Antibiotics reduce intestinal tumor development and change the gut microbiota composition. (**A**) Experimental protocols for treatment with antibiotics. Conventional Fabpl*Cre*;*Apc*$^{15lox/+}$ and *Apc*$^{15lox/+}$ mice (n = 14 and 6 per cohort, respectively) were monitored until examination of intestinal tumors at 22 weeks of age. FS, feces sample; *Ht*, *H.typhlonius*. Antibiotic treatment of the Abx embryo cohort started at embryonic day 11.5 feeding the pregnant mothers. (**B**) Intestinal tumor numbers in Fabpl*Cre*;*Apc*$^{15lox/+}$ mice of the NF cohort (n = 13), Abx pup cohort (n = 14) and Abx embryo cohort (n = 13). (**C**) Fabpl*Cre*;*Apc*$^{15lox/+}$ subcohorts in the *Ht*-positive Abx pup cohort with and without *A.muciniphila* (*Am*) (n = 6 and 8, respectively). (**D**) Intestinal tumor numbers of the two subcohorts of (C). (**E**) Hierarchical clustering of the MITChip data from two *Ht*/*Am*-positive conventional Fabpl*Cre*;*Apc*$^{15lox/+}$ mice of the NF cohort and two *Ht*/*Am*-negative Fabpl*Cre*;*Apc*$^{15lox/+}$ mice of the Abx embryo cohort (Pearson correlation). From all four mice FS1 was analyzed, and from one mouse of each category also FS5. (**F**) PCA using the MITChip data of (E). Mean tumor numbers ± SEM and significant differences according to *post hoc* ANOVA one-way statistical analysis are shown.*$P < 0.05$, **$P < 0.01$.

(Figure 3B). The average tumor area in both Abx cohorts was also reduced, but only significantly in the Abx pup cohort (P = 0.007) (Supplementary Figure 2A, available at *Carcinogenesis* Online).

Macroscopically, the tumor growth patterns of the antibiotic-treated and untreated mice were similar and mainly sessile (79 and 89%; n = 84 and 80). Microscopically, the tumors of both antibiotic-treated and untreated mice were nearly all adenomas (100 and 96%, respectively) and mainly composed of tubular structures lined by dysplastic epithelium.

Next, we investigated the effect of the early presence of *A.muciniphila* in the gut on intestinal tumor formation, because we observed that only a subset of Fabpl*Cre*; *Apc*$^{15lox/+}$ mice in the NF cohort and Abx pup cohort was positive for *A.muciniphila* (2/13 and 6/14, respectively) (Figure 3C). Apparently, although 1 week of cohousing was sufficient to transmit *H.typhlonius* from conventional to pathogen-low parental mice, transmission and establishment of *A.muciniphila* required a longer period of cohousing. In addition, we found that the antibiotic treatment eradicated not only *H.typhlonius* but also *A.muciniphila* (Supplementary Figure 1B, available at *Carcinogenesis* Online), and changed the abundance of other bacteria as well (see below). Remarkably, early presence of *A.muciniphila* was associated with halving of the mean intestinal tumor number (11.7 tumors in *H.typhlonius*- and *A.muciniphila*-positive mice versus 23.4 tumors in *H.typhlonius*-positive, *A.muciniphila*-negative mice (P = 0.018)), without influencing the average tumor area (Figure 3D and Supplementary Figure 2B, available at *Carcinogenesis* Online).

To investigate the effect of the antibiotic treatment on the global gut microbiota, we performed MITChip analysis on the feces of two mice of the NF cohort (those that were *H.typhlonius*- and *A.muciniphila*-positive) and two of the Abx embryo cohort (that were *H.typhlonius*- and *A.muciniphila*-negative). Hierarchical cluster analysis demonstrated that the two types of samples clustered separately (Figure 3E). PCA showed that among the taxa that correlated with the antibiotic treatment, and therefore with reduced tumor numbers, were members of the order *Clostridiales*, including *unclassified Clostridiales XIVa* (Figure 3F).

Intestinal tumor modulation by colonization with *H.typhlonius* and/or *A.muciniphila*

To test whether colonization of *H.typhlonius* and/or *A.muciniphila* was associated with intestinal tumor modulation, we introduced these bacteria directly into the stomach

of pathogen-low mice by triple gavage after 1 week of antibiotic pre-treatment (Figure 4A). Introduction proved to be effective for the *H.typhlonius*-only and *A.muciniphila*-only cohorts (Supplementary Figure 3A–C, available at *Carcinogenesis* Online). At 22 weeks of age, Fabpl*Cre*;*Apc*$^{15lox/+}$ mice, receiving just PBS, developed on average 13.6 intestinal tumors (Figure 4B). Both the *H.typhlonius* and *A.muciniphila* cohorts showed significantly more tumors: on average 20.1 ($P = 0.019$) and 23.5 ($P = 0.001$) (Figure 4B). Simultaneous colonization with *H.typhlonius* and *A.muciniphila* did not lead to dual colonization, but stable dual colonization was established by introduction of *A.muciniphila* in *H.typhlonius*-positive mice 2 weeks after *H.typhlonius* gavage (Supplementary Figure 3D, available at *Carcinogenesis* Online). Interestingly, this dual *H.typhlonius*/*A.muciniphila* cohort developed on average 14.8 intestinal tumors, comparable to the PBS cohort ($P = 0.642$) and significantly less than both the *H.typhlonius* ($P = 0.043$) and *A.muciniphila* cohorts ($P = 0.002$) (Figure 4B). The average tumor area was similar for all four cohorts (Supplementary Figure 4, available at *Carcinogenesis* Online).

To investigate the effect of colonization of *H.typhlonius* and/or *A.muciniphila* on the global gut microbiota composition, we performed MITChip analysis of three mice in each cohort. Hierarchical clustering did not show a clear separation between the samples of the four cohorts (data not shown). However, the PCA revealed that the microbiota composition of the *A.muciniphila* and *H.typhlonius* cohorts separated from the *H.typhlonius*/*A.muciniphila* and PBS cohorts (Figure 4C). The taxa correlating with PBS and dual colonization, i.e. with reduced tumor numbers, contained *Clostridiales*, including *unclassified Clostridiales XIVa* and *Bryantella et rel.* (Figure 4C).

The 15–27 tumors studied of each cohort were mainly adenomas (Supplementary Figure 5A–D, available at *Carcinogenesis* Online). The growth pattern was sessile, broad-based, pedunculated or polypoid. Most adenomas were histologically tubular with a large fraction composed of tubular structures lined by dysplastic epithelium. However, *H.typhlonius*, and/or *A.muciniphila* did not show colitis (histologic colitis score <1, see Supplementary Figure 5E, available at *Carcinogenesis* Online), indicating that colonization with these bacteria promoted non-colitis-associated tumorigenesis.

A.muciniphila has been shown to counteract the decreased thickness of the inner mucus layer in mice with high-fat diet-induced obesity (27). To investigate the impact of *A.muciniphila* and *H.typhlonius* on mucus layer thickness, we established a new series of *Apc*$^{15lox/+}$ and Fabpl*Cre*;*Apc*$^{15lox/+}$ mice, colonized these by triple gavages, and measured the inner mucus layer at 18–22 weeks (Figure 5A and C). PBS-treated Fabpl*Cre*;*Apc*$^{15lox/+}$ mice showed a thinner inner mucus layer than *Apc*$^{15lox/+}$ mice (12.3±1.3 and 18.6±3.4 µm, respectively), but this reduction was not significant ($P = 0.074$ by two-tailed Student *t* test). In Fabpl*Cre*;*Apc*$^{15lox/+}$ mice, *A.muciniphila* significantly increased the thickness from 12.3 to 19.2 µm (Figure 5A). *H.typhlonius* also increased mucus layer thickness, but less than *A.muciniphila* (15.4 µm). Dual colonization resulted in a significantly thinner mucus layer (13.3 µm) than with *A.muciniphila* alone, and more comparable to the PBS cohort. Overall, the inner mucus layer in

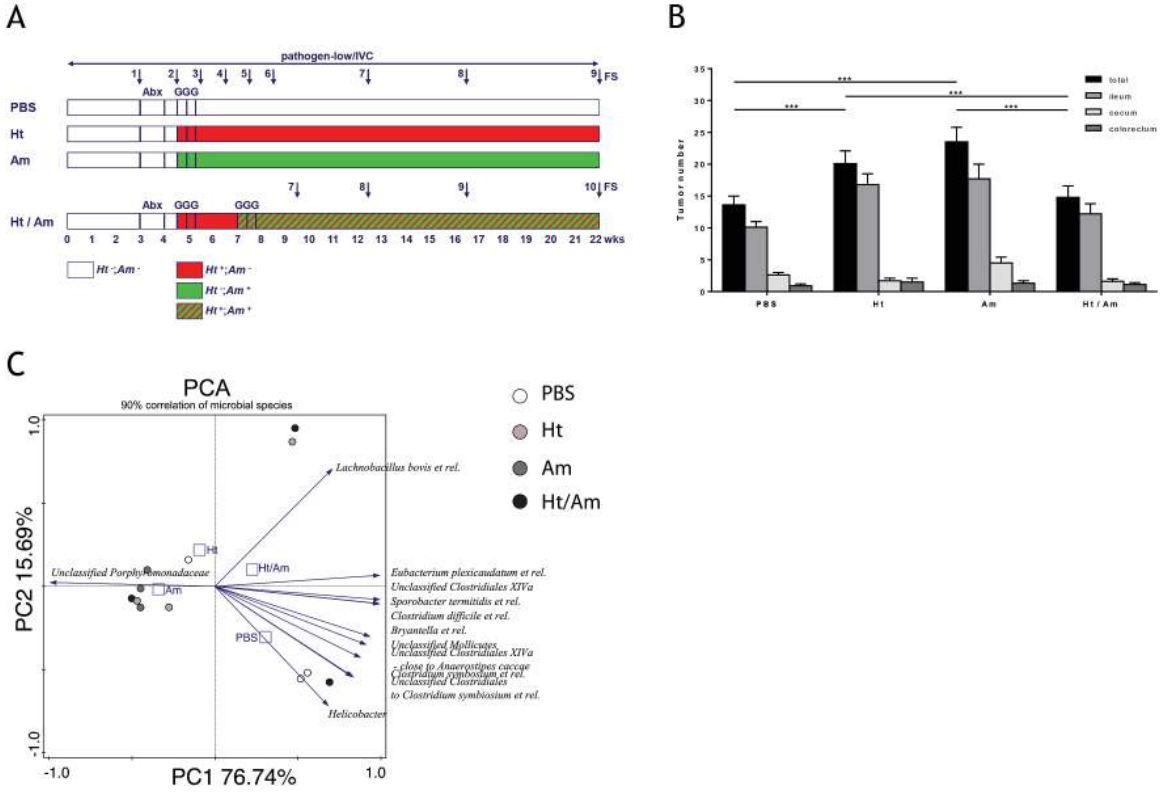

Figure 4. *H.typhlonius* and/or *A.muciniphila* colonization modulates intestinal tumor formation. (**A**) Experimental protocols for colonization of pathogen-low mice, pre-treated with antibiotics, with PBS, *H.typhlonius* (*Ht*), *A.muciniphila* (*Am*), *H.typhlonius* 2 weeks later followed by *A.muciniphila* (*Ht/Am*) by triple gavages (GGG). FS, feces sample. (**B**) Intestinal tumor numbers in Fabpl*Cre*;*Apc*$^{15lox/+}$ mice of the four cohorts: PBS ($n = 14$), *Ht* ($n = 18$), *Am* ($n = 13$) and *Ht/Am* ($n = 18$). (**C**) PCA using MITChip data from pathogen-low Fabpl*Cre*;*Apc*$^{15lox/+}$ mice of all four cohorts. Small square, nominal environmental variable. Mean tumor numbers ± SEM and significant differences according to *post hoc* ANOVA one-way statistical analysis are shown.***$P < 0.001$.

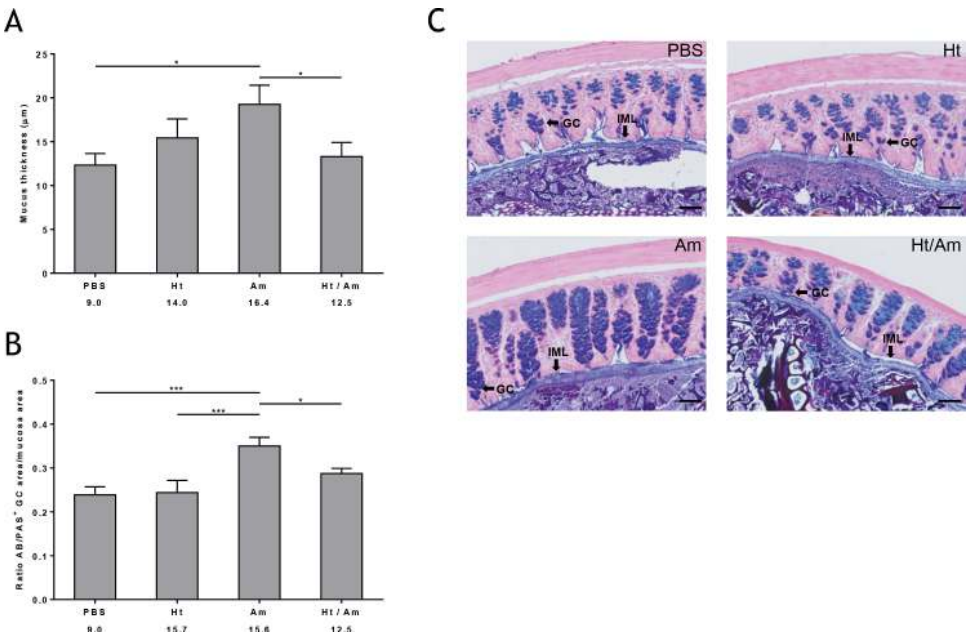

Figure 5. Mucus layer thickness and goblet cell number in colonized Fabpl*Cre*;*Apc*$^{15lox/+}$ mice correspond with tumor number. (**A**) Thickness of the mucus layer in sections stained with AB/PAS in Fabpl*Cre*;*Apc*$^{15lox/+}$ mice at 18–22 weeks of age (n = 7–8 per cohort). (**B**) Goblet cell number, defined as ratio AB/PAS^{+} goblet cell area/mucosa area in sections of Fabpl*Cre*;*Apc*$^{15lox/+}$ mice (n = 5–8 per cohort). Mean mucus thicknesses and ratios AB/PAS^{+} goblet cell area/mucosa area ± SEM are shown. Data are significant according to *post hoc* ANOVA one-way statistical analysis. *P < 0.05, ***P < 0.001. Corresponding average tumor numbers in these cohorts are indicated. (**C**) Representative AB/PAS-stained images for mucus layer thickness and goblet cell measurements. GC, goblet cells; IML, inner mucus layer. Scale bar = 50 µm.

the Fabpl*Cre*;*Apc*$^{15lox/+}$ cohorts followed the pattern of the average tumor count in these cohorts (Figure 5A).

Since mucus layer thickness is largely dependent on the number of mucus-producing goblet cells, we also investigated the goblet cell density (defined as the ratio between the goblet cell area and the mucosa area) in these mice. The Fabpl*Cre*;*Apc*$^{15lox/+}$ and *Apc*$^{15lox/+}$ PBS mice showed comparable goblet cell ratios (0.24 ± 0.02 and 0.26 ± 0.02). *A.muciniphila* significantly increased the goblet cell ratio relative to PBS (0.35 versus 0.24), and dual colonization (0.35 versus 0.29), whereas *H.typhlonius* colonization did not affect the goblet cell ratio (Figure 5B). Except for the *H.typhlonius* cohort, the number of goblet cells in the Fabpl*Cre*;*Apc*$^{15lox/+}$ mice corresponded with the inner mucus layer thickness and also with the average tumor count (Figure 5B).

Discussion

This study was based on our observation that transfer of intestinal tumor-prone Fabpl*Cre*;*Apc*$^{15lox/+}$ mice from conventional to pathogen-low housing conditions was accompanied by a significant decrease in the number of colorectal tumors. Considering that housing differences might change the mouse microbiota, we characterized these by metagenomic sequencing of the stool of mice kept under both conditions. These studies identified *H.typhlonius* and *A.muciniphila* as specifically associated with conventional housing. Our data corroborated the impact of different animal housing conditions on gut microbiota and on tumor load of *Apc* mutant mice (15,37).

We showed that *H.typhlonius* can act as a pathogen in immune-competent mice, because single *H.typhlonius* colonization of pathogen-low Fabpl*Cre*;*Apc*$^{15lox/+}$ mice increased the number of intestinal tumors. Antibiotic eradication of *H.typhlonius* in conventionally housed mice reduced both tumor count and size, further supporting the pathogenic role of this species in intestinal tumor development. This tumor-promoting role in immune-competent mice is remarkable. *H.typhlonius* has been described as a pathobiont, a benign commensal in immune-competent animals and only an opportunistic pathogen in immune-compromised *Il10*$^{-/-}$ mice, where it causes severe typhlocolitis and colitis-associated neoplasia (24,26). Likewise, the closely related species *H.hepaticus* and *H.bilis* cause inflammation-mediated colon tumorigenesis in immune-compromised *Rag2*$^{-/-}$ and *Smad3*$^{-/-}$ mice (10–14). Conflicting data exist with regard to the tumor-promoting role of *Helicobacter* infection in immune-competent *Apc*$^{Min/+}$ mice. In one study, the combined infection of *H.hepaticus* and *H.bilis* did not result in the promotion of intestinal adenoma formation (11). However, in another study an increase in intestinal adenoma multiplicity upon *H.hepaticus* infection was noted (12). Our finding that *H.typhlonius* colonization of immune-competent Fabpl*Cre*;*Apc*$^{15lox/+}$ mice increased the number of intestinal tumors is in accordance with the latter observation.

A.muciniphila is a mucin-degrading bacterium (25). It is the single intestinal representative of the phylum Verrucomicrobia, and present at high numbers in the intestinal tract of healthy humans (abundance of 1–4% in colon). Its abundance inversely correlates with body weight, and the occurrence of several intestinal disorders including inflammatory bowel disease, diabetes, obesity, and appendicitis (36). Recent studies showed a beneficial role of *A.muciniphila*. For instance, *A.muciniphila* treatment reversed high-fat diet-induced metabolic disorders in mice, including adipose tissue inflammation and counteracted the diet-induced decrease in mucus layer and number of goblet cells (27,38). In another study, *A.muciniphila* colonization of gnotobiotic mice was shown to increase the number of mucus-producing goblet cells in cecum and colon (39). On the other hand, *A.muciniphila* was increased in a T-cell transfer-mediated mouse model of intestinal inflammation, and decreased in *Il10*$^{-/-}$ mice after colonization with the probiotic bacterium *Enterococcus faecium* NCIMB 10415, associated with reduced inflammation (40,41). Moreover, *A.muciniphila*

colonization of gnotobiotic mice exacerbated *Salmonella thyphimurium*-induced intestinal inflammation by its ability to disturb host mucus homeostasis (39). This suggests that the role of *A.muciniphila* may be host- and condition-dependent.

Little is known about the relationship between *A.muciniphila* and intestinal cancer. A 4-fold higher abundance was found in the stool of CRC patients as compared to healthy subjects (42). *Akkermansia* was likewise found to be significantly increased in mucosal biopsy samples of patients with colorectal adenomas (43). However, several studies in man, mice and other model systems have shown that food intake reduction results in a significantly increased relative amount of *A.muciniphila* or related bacteria (44). As it is known that CRC patients have a reduced food intake, meaningful interpretations of the intestinal microbiome associations await incorporation of dietary information in the analysis. In a mouse model of inflammation-associated CRC, enrichment for *A.muciniphila* genera was noted in the fecal content of tumor-bearing mice (45). Recently, these authors reported that *Akkermansia* (together with members of *Bacteroides*) showed a positive correlation with increased inflammation-associated colonic tumor burden in contrast to members of *Clostridiales*, including multiple members of *Clostridium* group XIVa (46). We note that, unlike our intervention studies, these findings may be reactive rather than causal. Our colonization experiments revealed a positive role for *A.muciniphila* and for *H.typhlonius* on tumor development of Fabpl*Cre*;*Apc*$^{15lox/+}$ mice (Figure 4A and B). Unsupervised cluster analysis by PCA demonstrated that multiple members of *unclassified Clostridiales* positively correlated with the *H.typhlonius*/*A.muciniphila* and control colonizations, i.e. with conditions of decreased tumor burden (Figure 4C). The positive association of *A.muciniphila* (and of *H.typhlonius*) and the negative association of *unclassified Clostridiales* with increased tumor burden was also apparent in the conventional—pathogen-low and NF—Abx embryo comparisons (Figures 2C and 3F, respectively). Except for *Bacteroidales*, which did not emerge from our PCAs, these results are consistent with the recent findings in inflammation-associated CRC, showing that *Akkermansia* and *Bacteroidales* were correlated with exacerbated tumorigenesis and *Clostridiales* with tumor protection (46).

The increased tumor count after colonization with *A.muciniphila* (and also with *H.typhlonius*) was accompanied by an increase of the mucus layer and goblet cell density. The latter effects of *A.muciniphila* were also reported by others for obese mice (27,38). However, although *A.muciniphila* counteracted the thinning of the mucus layer in both our tumor-prone mice and the described obese mice, it counteracted the obesity, while exacerbating the intestinal tumor phenotype. Thus, our data suggest that restoration by *A.muciniphila* of the thickness of the mucus layer (as a gut barrier) to normal levels in healthy mice, appears to aggravate the disease in tumor-prone mice. This unexpected phenomenon needs to be further investigated. Single colonization with *H.typhlonius* also caused a (non-significant) increase in mucus layer thickness in Fabpl*Cre*;*Apc*$^{15lox/+}$ mice, but no increase in goblet cell density.

One would expect that co-colonization of both tumor-promoting bacterial species would lead to exacerbation, instead of the observed reduction, of intestinal tumor formation and to a further increase, instead of a decrease, in mucus layer thickness and goblet cell density. Apparently, *A.muciniphila* or *H.typhlonius* act differently upon joint colonization, indicative of a dualistic effect of these bacteria in concert with the host genetic background. In case of *A.muciniphila*, the possible dual effect on goblet cell density is reminiscent of recent findings in gnotobiotic mice, showing that *A.muciniphila* increased the number of goblet cells, but upon co-colonization exacerbated the decrease of goblet cell number by *Salmonella thyphimurium* (39).

In conclusion, our work shows that *A.muciniphila* and *H.typhlonius* are prime candidates for microbiota-borne modulation of intestinal tumorigenesis, even while the complex antagonism and interaction with the host clearly needs further study. Investigation of the effect of *A.muciniphila* and/or *H.typhlonius* colonization on the gut immune system and permeability, and the metabolite production of the gut microbiota could prove valuable.

Supplementary material

Supplementary Table 1 and Supplementary Figures 1–5 can be found at http://carcin.oxfordjournals.org/

Funding

Valorization Fund of the Centre for Medical Systems Biology (to E.C.R.-M.), the Netherlands Organization for Scientific Research (Spinoza Award and SIAM Gravity Grant to W.M.deV.); the European Research Council (ERC Advanced Grant 250172 MicrobesInside to W.M.deV.).

Acknowledgements

We thank Victor C.L. de Jager for bioinformatics assistance, Wieke de Bruin and Els van Oorschot for advice on bacterial cultures, Steven Aalvink for providing the *A.muciniphila* stocks, Ben van der Geest and Fred de Boer for biotechnical assistance, Saskia Maas and Jan Leeflang for advice on histopathology, Bruno Sovran and Jan Dekker for advice on mucus layer analysis and Theo Hulsebos for critically reading the manuscript.
Conflict of Interest Statement: None declared.

References

1. Qin, J. et al. (2010) A human gut microbial gene catalogue established by metagenomic sequencing. Nature, 464, 59–65.
2. Lozupone, C.A. et al. (2012) Diversity, stability and resilience of the human gut microbiota. Nature, 489, 220–230.
3. Arthur, J.C. et al. (2011) The struggle within: microbial influences on colorectal cancer. Inflamm. Bowel Dis., 17, 396–409.
4. Kabir, S. (2009) Effect of *Helicobacter pylori* eradication on incidence of gastric cancer in human and animal models: underlying biochemical and molecular events. Helicobacter, 14, 159–171.
5. Boleij, A. et al. (2012) Gut bacteria in health and disease: a survey on the interface between intestinal microbiology and colorectal cancer. Biol. Rev. Camb. Philos. Soc., 87, 701–730.
6. Garrett, W.S. et al. (2009) Colitis-associated colorectal cancer driven by T-bet deficiency in dendritic cells. Cancer Cell, 16, 208–219.
7. Uronis, J.M. et al. (2009) Modulation of the intestinal microbiota alters colitis-associated colorectal cancer susceptibility. PLoS One, 4, e6026.
8. Wu, S. et al. (2009) A human colonic commensal promotes colon tumorigenesis via activation of T helper type 17 T cell responses. Nat. Med., 15, 1016–1022.
9. Arthur, J.C. et al. (2012) Intestinal inflammation targets cancer-inducing activity of the microbiota. Science, 338, 120–123.
10. Erdman, S.E. et al. (2003) CD4+ CD25+ regulatory T lymphocytes inhibit microbially induced colon cancer in Rag2-deficient mice. Am. J. Pathol., 162, 691–702.
11. Maggio-Price, L. et al. (2006) Helicobacter infection is required for inflammation and colon cancer in SMAD3-deficient mice. Cancer Res., 66, 828–838.
12. Rao, V.P. et al. (2006) Innate immune inflammatory response against enteric bacteria *Helicobacter hepaticus* induces mammary adenocarcinoma in mice. Cancer Res., 66, 7395–7400.
13. Nagamine, C.M. et al. (2008) *Helicobacter hepaticus* infection promotes colon tumorigenesis in the BALB/c-Rag2(-/-) Apc(Min/+) mouse. Infect. Immun., 76, 2758–2766.

14. Erdman, S.E. et al. (2009) Nitric oxide and TNF-alpha trigger colonic inflammation and carcinogenesis in *Helicobacter hepaticus*-infected, Rag2-deficient mice. Proc. Natl. Acad. Sci. USA, 106, 1027–1032.
15. Li, Y. et al. (2012) Gut microbiota accelerate tumor growth via c-jun and STAT3 phosphorylation in APCMin/+ mice. Carcinogenesis, 33, 1231–1238.
16. Dulal, S. et al. (2014) Gut microbiome and colorectal adenomas. Cancer J., 20, 225–231.
17. Marchesi, J.R. et al. (2011) Towards the human colorectal cancer microbiome. PLoS One, 6, e20447.
18. Castellarin, M. et al. (2012) *Fusobacterium nucleatum* infection is prevalent in human colorectal carcinoma. Genome Res., 22, 299–306.
19. Kostic, A.D. et al. (2012) Genomic analysis identifies association of Fusobacterium with colorectal carcinoma. Genome Res., 22, 292–298.
20. Kostic, A.D. et al. (2013) *Fusobacterium nucleatum* potentiates intestinal tumorigenesis and modulates the tumor-immune microenvironment. Cell Host Microbe, 14, 207–215.
21. Robanus-Maandag, E.C. et al. (2010) A new conditional Apc-mutant mouse model for colorectal cancer. Carcinogenesis, 31, 946–952.
22. Koelink, P.J. et al. (2009) 5-Aminosalicylic acid inhibits colitis-associated but not sporadic colorectal neoplasia in a novel conditional Apc mouse model. Carcinogenesis, 30, 1217–1224.
23. Fox, J.G. et al. (1999) A novel urease-negative Helicobacter species associated with colitis and typhlitis in IL-10-deficient mice. Infect. Immun., 67, 1757–1762.
24. Franklin, C.L. et al. (2001) *Helicobacter typhlonius* sp. nov., a Novel Murine Urease-Negative Helicobacter Species. J. Clin. Microbiol., 39, 3920–3926.
25. Derrien, M. et al. (2004) *Akkermansia muciniphila* gen. nov., sp. nov., a human intestinal mucin-degrading bacterium. Int. J. Syst. Evol. Microbiol., 54(Pt 5), 1469–1476.
26. Chichlowski, M. et al. (2008) *Helicobacter typhlonius* and *Helicobacter rodentium* differentially affect the severity of colon inflammation and inflammation-associated neoplasia in IL10-deficient mice. Comp. Med., 58, 534–541.
27. Everard, A. et al. (2013) Cross-talk between *Akkermansia muciniphila* and intestinal epithelium controls diet-induced obesity. Proc. Natl. Acad. Sci. USA, 110, 9066–9071.
28. Out, A.A. et al. (2009) Deep sequencing to reveal new variants in pooled DNA samples. Hum. Mutat., 30, 1703–1712.
29. Altschul, S.F. et al. (1990) Basic local alignment search tool. J. Mol. Biol., 215, 403–410.
30. Mitra, S. et al. (2009) Visual and statistical comparison of metagenomes. Bioinformatics, 25, 1849–1855.
31. Feng, S. et al. (2005) Differential detection of five mouse-infecting helicobacter species by multiplex PCR. Clin. Diagn. Lab. Immunol., 12, 531–536.
32. Collado, M.C. et al. (2007) Intestinal integrity and *Akkermansia muciniphila*, a mucin-degrading member of the intestinal microbiota present in infants, adults, and the elderly. Appl. Environ. Microbiol., 73, 7767–7770.
33. Everard, A. et al. (2011) Responses of gut microbiota and glucose and lipid metabolism to prebiotics in genetic obese and diet-induced leptin-resistant mice. Diabetes, 60, 2775–2786.
34. Geurts, L. et al. (2011) Altered gut microbiota and endocannabinoid system tone in obese and diabetic leptin-resistant mice: impact on apelin regulation in adipose tissue. Front. Microbiol., 2, 149.
35. Derrien, M. et al. (2008) The Mucin degrader *Akkermansia muciniphila* is an abundant resident of the human intestinal tract. Appl. Environ. Microbiol., 74, 1646–1648.
36. Belzer, C. et al. (2012) Microbes inside–from diversity to function: the case of Akkermansia. ISME J., 6, 1449–1458.
37. Colnot, S. et al. (2004) Colorectal cancers in a new mouse model of familial adenomatous polyposis: influence of genetic and environmental modifiers. Lab. Invest., 84, 1619–1630.
38. Shin, N.R. et al. (2014) An increase in the Akkermansia spp. population induced by metformin treatment improves glucose homeostasis in diet-induced obese mice. Gut, 63, 727–735.
39. Ganesh, B.P. et al. (2013) Commensal *Akkermansia muciniphila* exacerbates gut inflammation in *Salmonella typhimurium*-infected gnotobiotic mice. PLoS One, 8, e74963.
40. Stecher, B. et al. (2007) *Salmonella enterica* serovar typhimurium exploits inflammation to compete with the intestinal microbiota. PLoS Biol., 5, 2177–2189.
41. Ganesh, B.P. et al. (2012) *Enterococcus faecium* NCIMB 10415 does not protect interleukin-10 knock-out mice from chronic gut inflammation. Benef. Microbes, 3, 43–50.
42. Weir, T.L. et al. (2013) Stool microbiome and metabolome differences between colorectal cancer patients and healthy adults. PLoS One, 8, e70803.
43. Sanapareddy, N. et al. (2012) Increased rectal microbial richness is associated with the presence of colorectal adenomas in humans. ISME J., 6, 1858–1868.
44. Salonen, A. et al. (2014) Impact of diet on human intestinal microbiota and health. Annu. Rev. Food Sci. Technol., 5, 239–262.
45. Zackular, J.P. et al. (2013) The gut microbiome modulates colon tumorigenesis. MBio, 4, e00692–e00613.
46. Baxter, N.T. et al. (2014) Structure of the gut microbiome following colonization with human feces determines colonic tumor burden. Microbiome, 2, 20.